Int. J. Nanosci. Nanotechnol., Vol. 14, No. 3, Sept. 2018, pp. 197-206

Investigation on Microstructure, Lattice and Structural Chemistry of Biogenic Silver Nanoparticles

Saeed Jafarirad[1,*], Milad Kordi[1] and Morteza Kosari-Nasab[2]

[1]Department of phytochemistry, Research Institute for Fundamental Sciences (RIFS), University of Tabriz, Tabriz, Iran.
[2]Drug Applied Research Center, Tabriz University of Medical Sciences, Tabriz, Iran.

(*) Corresponding author: jafarirad@tabrizu.ac.ir
(Received: 10 December 2015 and Accepted: 21 February 2018)

Abstract

The use of plant extract in the biosynthesis of nanoparticles (NPs) can be an eco-friendly approach and have been suggested as a possible alternative to classic methods namely physical and chemical procedures. This study was designed to examine the structural chemistry of silver nanoparticles (AgNPs) using both conventional heating and microwave irradiation methods. To our knowledge, this is the first report that proposes a structural chemistry during synthesis of biogenic silver nanoparticles using Artemisia fragrans extracts. The as-synthesized AgNPs by both approaches were characterized using UV-vis, FTIR, XRD, SEM, EDX, DLS with zeta potential analysis and antioxidant activity. Characterization data revealed that AgNPs produced by microwave irradiation (900 W) and conventional heating (100ºC) have average size of 18.06 (zeta potential, -46) and 60.08 nm (zeta potential, -39), respectively. The synthesis of such biogenic AgNPs using eco-friendly reagents in minimum time open the road for decreasing cytotoxicity of the AgNPs without risking interference of toxic chemical agents. In addition, this eco-friendly synthesis with green approach is a new, cheap, and convenient technique suitable for both commercial production and health related applications of AgNPs.

Keywords: *Nanoparticles, Structural chemistry, Synthesis, Bio-nano structure.*

1. INRODUCTION

Nowadays, the noble metal nanoparticles (NPs) demonstrate new optical, electronical and physicochemical properties which are observed neither in the individual molecules nor in the bulk metals. Among noble metal nanoparticles, AgNPs have many applications in medicine [1, 2] drug delivery [3], food industries [4], agriculture [5], textile industries [6], water treatment [7] and as the antimicrobial and antifungal agents [8, 9].

The cost-effective production of NPs having good phase selectivity, crystallinity and particle size homogeneity is still a challenge to scientists. Currently, a large number of physical, chemical and hybrid methods have been reported to synthesize different types of NPs such as photo reduction [10], laser ablation [11], chemical reduction [12] and chemical vapor deposition [13]. However, most of these methods are expensive, high energy requirement, cause potential environmental and biological hazards, consumption organic solvents or toxic reducing agents, and low yields of production [14, 15]. Therefore, there is an increasingly need to develop nontoxic, low cost, clean and compatible with the principles of green chemistry procedures for producing NPs. These biological systems including plant extracts [16-18], yeast [19] have been reported to produce various kinds of NPs. The use of plant extracts for producing NPs is quickly developing due to their growing success and ease of NPs formation [20, 21].

Artemisia L. (Asteraceae) is a large genus of bitter aromatic herbs or shrubs consisting of over 350 species. Artemisia

fragrans Willd. (A. fragrans Willd.), commonly known as Chao, grows in Iran, Russia and neighboring areas, and is famed for its strong fragrance [22]. Several biological activities have been reported for Artemisia species, including anti-malarial, antiviral, anti-tumor, anti-pyretic, anti-hemorrhagic, anticoagulant, anti-anginal, anti-oxidant, anti-hepatitis, anti-ulcerogenic and antispasmodic properties [23].

On the other hands, studies in the field of medicine have shown that silver is effective against for more than 650 pathogens, having a broad spectrum of activity. Its use in the form of nanoparticles enhances this property, allowing its use in a wide range of applications [24]. Hence, in the present paper we used A. fragrans Willd extract as both reducing and capping agents in order to have a synergistic effect on medical applications of as-synthesized AgNPs potentially. In this direct, we described for the first time, the extracellular biosynthesis and characterization of AgNPs using fruit extraction of A. fragrans Willd. Moreover, the comparison between both conventional heating (CH) and microwave irradiation (MI) methods to synthesize AgNPs has been investigated. In addition, the possible mechanism of biosynthesis, as a green technique, has been proposed.

2. EXPERIMENTAL PROCEDURE

2.1. Materials and Methods

All the chemical reagents used in this experiment were of analytical grade. The leaves of fresh *A. fragrans Willd.* were collected from Bostanabad city, the county with an area of 2795 km² which is approximately spread at 37°51′N 46°50′E of east Azerbaijan province, Iran.

2.2. Scanning Electron Microscopy (SEM) and Energy Dispersive X-ray (EDX)

The SEM instrument MIRA3 FEG-SEM (Czech Republic) used to recognize the morphology and elemental analysis of the AgNPs.

2.3. Fourier Transform Infrared Spectroscopy (FTIR)

FTIR spectrum was recorded by TENSOR 27, Brucker (Germany) in the range of 400–4000 cm^{-1}. The AgNPs and the extract were analyzed in the form of powder using KBr.

2.4. X-Ray Diffraction (XRD)

XRD patterns of AgNPs was obtained using a powder X-ray diffractometer, Siemens (Germany) with Cu Kα radiations (k=1.54060 nm) in 2θ range from 20° to 80°. Data were analyzed using Origin Pro 9.1.0 SRO software (Orgin Lab Corporation, USA).

2.5. Dynamic Light Scattering (DLS) and Zeta Potential Measurement

Particle size and particle size distribution were evaluated using DLS Nanotrac Wave, Microtrac Company. All experiments were done in triplicates to check for accuracy. The zeta potential of as-synthesized AgNPs was determined in water.

2.6. Preparation of Leaf and Stem Extract of *A. fragrans Willd.*

The leaf and stem were dried at room temperature at shade and then powdered. 20 g of this powder were added to 200 ml of water and placed on a shaker for 24 h at 60 °C. Then, it was filtered through Whatman No. 1 filter paper. The filtered extract was stored in the refrigerator at 4 °C for further studies.

2.7. Antioxidant Assay of the Extract using 1-diphenyl-1-2-picrylhydrazyl (DPPH)

The AgNPs and extract of *A. fragrans Willd.* were evaluated in respect of free radical scavenging activity by DPPH method. The scavenging activity on the DPPH radical was determined by measuring the absorbance at 517 nm by a UV-Vis spectrophotometer.

Radical scavenging activity was calculated using the formula (1):

$$\%I = (A_{control} - A_{sample}) / A_{control} \times 100 \quad (1)$$

where %I is percentage of radical scavenging activity, $A_{control}$ stands for the absorbance of the control sample (DPPH solution without test sample) and A_{test} is the absorbance of the test sample (DPPH solution with test compound). All tests were performed in triplicate and the results were averaged.

2.8. Extracellular Biosynthesis of AgNPs using CH Technique

In a typical synthesis of AgNPs, 5 ml of *A. fragrans Willd.* leaf and stem extract was added into the 50 ml of 0.01 M aqueous $AgNO_3$ solution then stirred and heated at 100 ºC for 30 min. In order to study the effect of temperature on the formation of AgNPs, the experiments are conducted at 25, 40, 60 and 80 ºC. The reduction of silver ions was monitored by measuring the absorbance of the solutions mixture of heating and microwave irradiation synthesis in a range of wavelength from 300 to 700 nm using UV–vis spectroscopy. The distilled water was used as a blank. Further, the obtained solution mixtures were centrifuged at 10,000 rpm for 15 min. Then a process of centrifugation and re-dispersion in the distilled water in the distilled water was repeated three times to ensure the complete separation of the AgNPs. The purified pellets were then kept in the oven for drying at 60 ºC for 24 h.

2.9. Extracellular Synthesis of AgNPs using MI Technique

Analytical grade of $AgNO_3$ was dissolved in the extract solution according to CH method except that the mixture was placed under microwave irradiation at 180, 360, 540 and 720 W during 3 minutes. Finally, the obtained pellets were heated according to the above-mentioned process (CH method) in air heated furnace.

3. RESULTS AND DISCUSSION

The synthesis of AgNPs could visually detect due to the color change of the extract on mixing with silver salt before and after biosynthesis stage due to reduction of Ag^+ to Ag^0 (Figure 1). In next section this issue would be discussed in detail (under subtitle of possible mechanism).

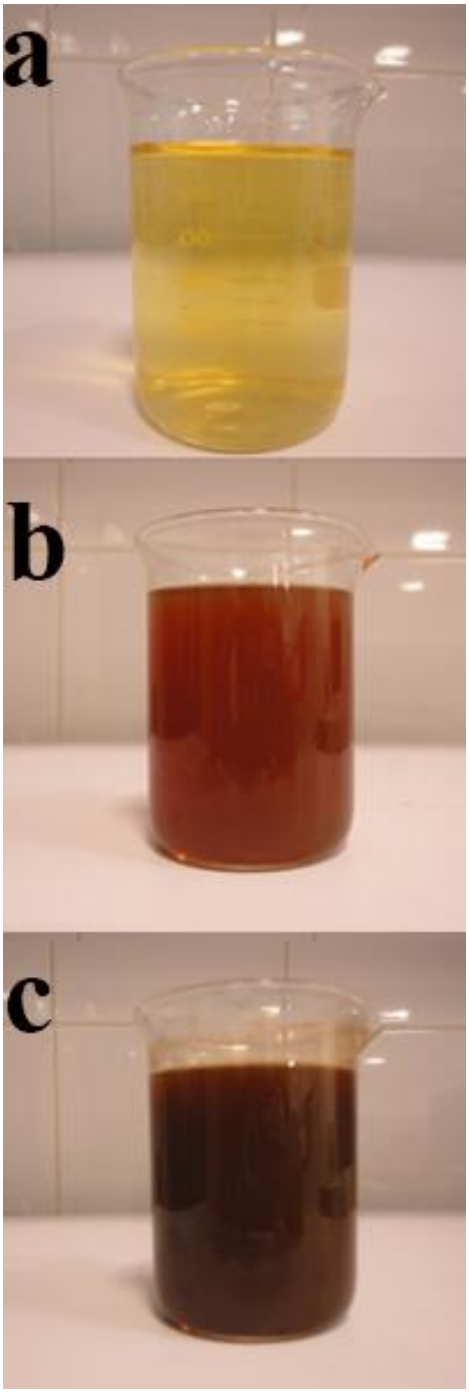

Figure 1. *Color change from light yellow to dark brown during the phytoreduction of silver nitrate to AgNPs; (a) Mixed solution*

before reaction (b) CH (100ºC) and (c) MI (900 W) approaches.

3.1. UV–vis Spectral Studies

The formation of AgNPs was first confirmed using UV-vis spectroscopy technique. The other reports mentioned that maximum absorbance occurred at 435 nm due to presence of AgNPs [25]. In CH method os synthesis the λ_{max} of as-synthesized samples placed at 449, 447, 446 and 444 nm for temperatures 40, 60, 80 and 100 ºC, respectively. It confirms the presence of AgNPs (Figure 2 a). In MI technique the λ_{max} of samples placed at 454, 434, 426 and 412 nm for powers of 360, 540, 720 and 900 W, respectively (Figure 2 b). It must be pointed out that the only exception in both methods were the temperature of 25 ºC (CH method) and power of 180 W (MI method), because in these cases the temperature and power were not sufficient to fabricate AgNPs.

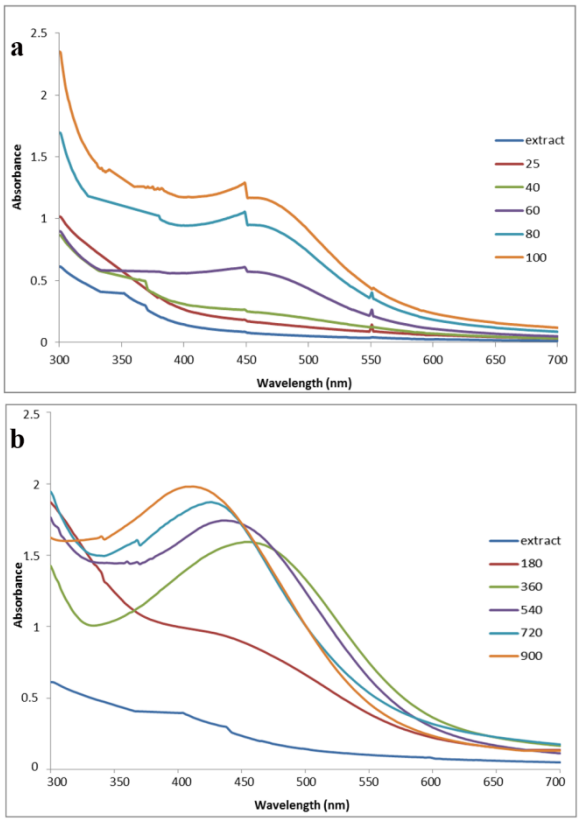

Figure 2. *UV-vis absorption spectra of AgNPs as a function of (a) temperature (CH) and (b) power levels (MI).*

The UV–vis absorption spectra showed that the increasing both of temperature (CH) and power (MI) lead to enhance in intensity of the adsorption peaks. It could be attributed to fact that, the energy absorption of the solution becomes greater, accordingly the reaction time becomes shorter, and finally the amount of nucleation increases [25]. Moreover, the increase of the microwave power (MI) cause a blue shift in the characteristic surface plasmon resonance band of AgNPs from 454 to 412 nm. Thus, the size of AgNPs became smaller which resulted in sharpness of surface plasmon resonance [26].

3.2. Morphological Properties

The SEM micrographs was confirmed that the AgNPs presence in both approaches were in Nano-size with diameter range of 25-131 and 17–76 nm for CH and MI methods, respectively. However, the NPs that synthesized using CH method are spherical while their counterparts that synthesized by MI possess irregular shapes (Figure 3).

3.3. Investigation on Colloidal Properties

We investigated the effect of both methods of synthesis on the particle size and the polydispersity index (PDI) using DLS technique. The average sizes of the AgNPs produced by the CH (at 100ºC) and MI (at 900 W) techniques were 60.08 and 18.06 nm, respectively (Figure 4).

Based on Table 1, the data exhibited the effect of source temperature by CH and power by MI on the formation of AgNPs with fairly well-defined diameter under 100 nm. In addition, with increasing both temperature and power, the energy absorption of the solution becomes greater and nucleation increases. Accordingly it reduce the size of the AgNPs [25]. Furthermore, due to the short time of synthesis in MI method (3 min), particle sizes of the synthesized AgNPs are smaller than their counterparts in CH technique.

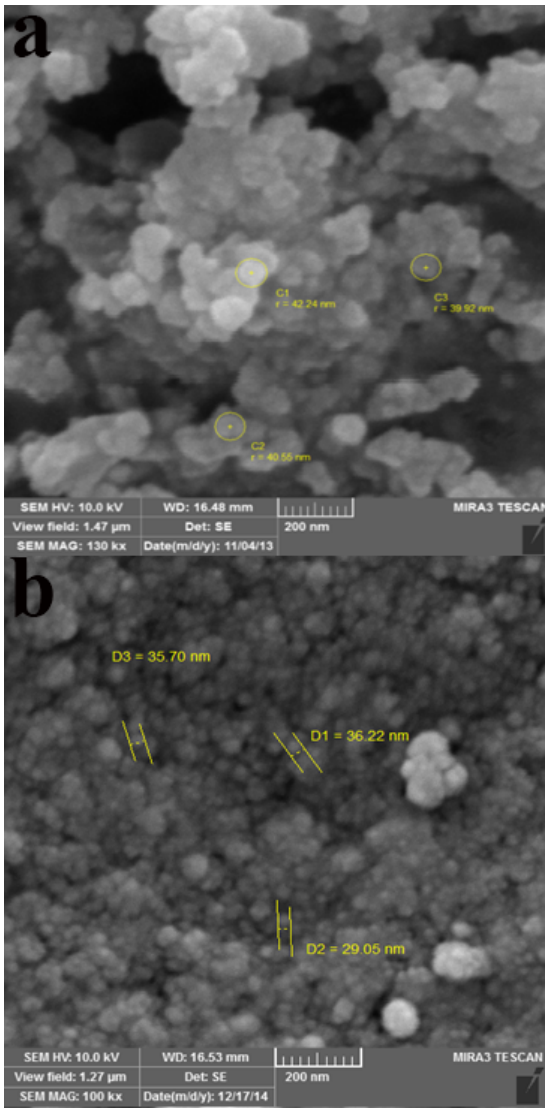

Figure 3. *SEM images of AgNPs prepared by a) CH method and b) MI method.*

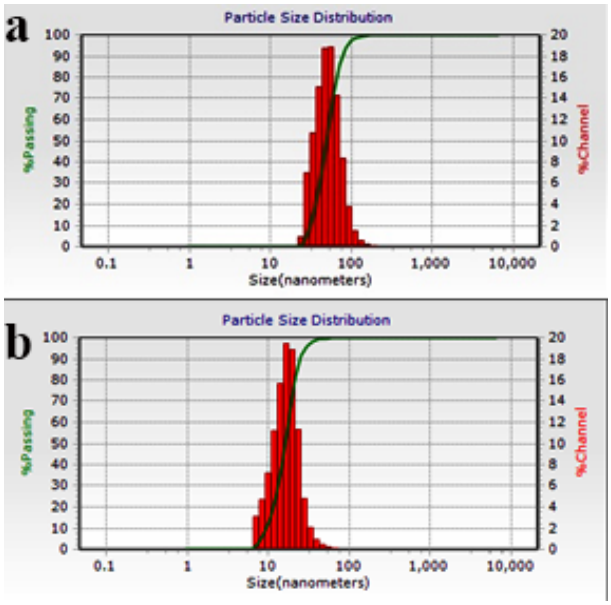

Figure 4. *DLS of AgNPs, a) CH (100ºC), and b) MI (900 W).*

Table1. *Effect of temperature (CH) and power (MI) on the formation of AgNPs.*

CH (ºC)[a]	MI (W)[b]	λ_{max} (nm)[c]	D(nm)[d]	Z (mV)[e]
40	-	444	75.06	-31
60	-	446	71.09	-25
80	-	447	65.41	-28
100	-	449	60.08	-39
-	360	454	60.12	-27
-	540	434	38.91	-36
-	720	426	23.14	-30
-	900	412	18.06	-46

[a]Source as chemical heating (CH method)
[b]Source as microwave irradiation (MI method)
[c]λ_{max}: maximum absorbance based on UV-vis spectroscopy
[d]D: Hydrodynamic diameter measured by DLS in water
[e]Z: zeta potential

The zeta potential of the synthesized AgNPs was determined in water as dispersant. Based on DLVO theory, the high absolute zeta potential value specifies a strong repulsive force among the particles which prevents aggregation. Therefore, in both methods, the high negative value confirms the repulsion among the particles and thereby increases in stability of the formulation.

3.4. XRD Pattern

The XRD peaks at 2θ = 27.88º, 32.29º, 38.13, 46.30º, 64.46º, 67.59º and 76.93º corresponding to the 210, 264, 111, 231, 220, 112 and 311 (CH, 100 ºC) and 27.88º, 32.32º, 38.25º, 46.29º, 64.56º and 76.95º corresponding to the 210, 122, 111, 231, 220 and 311 (MI, 900 W) planes, respectively (Figure 5).

The XRD pattern of the as-synthesized AgNPs using CH and MI was identical to a face-centered-cubic (fcc) structure [27, 28].

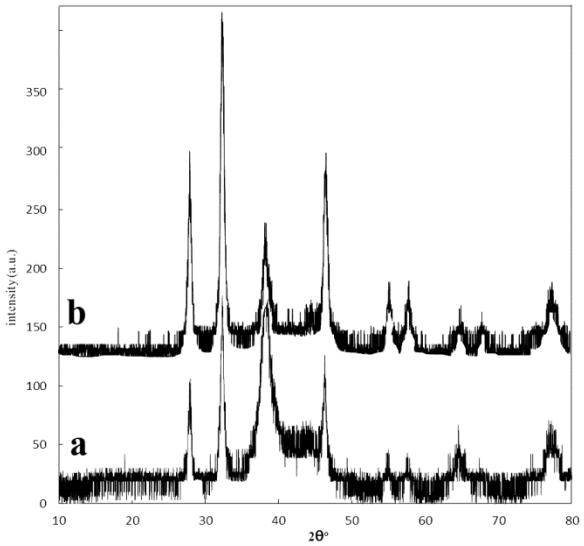

Figure 5. *XRD pattern of AgNPs, a) CH (100ºC), and b) MI (900 W).*

These patterns indicate that the peaks of AgNPs synthesized by CH method are narrower than the sample synthesized by MI, which is compatible with the SEM and DLS data. The sharpening of the peak clearly showed that the crystalline nature of the synthesized AgNPs by both methods. However, in MI method the crystal structure of AgNPs was not completed because the low time of synthesis (3 min). The average particle size has been estimated using the well-known Scherrer formula:

$d=K\lambda/\beta\cos\theta$ Eq. 1

where D stands for the particle diameter, κ is a constant equals 0.89, λ is the wavelength of X-ray source (0.1541 nm), β is the full width at half maximum (FWHM) and θ is the diffraction angle. The calculated particle sizes were 45.08 and 15.25 nm for CH and MI methods, respectively (Table 2).

Table 2. *Colloidal properties of AgNPs for both CH and MI methods.*

CH (ºC)	MI (W)	D (nm)			PDI (μ_2/T^2)[d]	Z[e] (mV)
		XRD[a]	SEM[b]	DLS[c]		
100	-	13.3	25-131	60.08	0.884	-39
-	900	11.3	7–76	18.06	1.021	-46

[a] Theoretical diameter calculated by Origin software based on Scherrer's equation

[b] Particle mean diameter measured by SEM

[c] Hydrodynamic diameter measured by DLS in water

[d] Polydispersity index based on DLS

[e] zeta potential

3.5. EDX Profile

The EDX spectrum of AgNPs by MI (900 W) method was indicated in Figure 6 as a typical sample. Metallic silver nanocrystals generally show typical optical absorption peak approximately at 2.98 keV [29]. There were also observed spectral signals for carbon, chlorine and oxygen indicated that the organic compounds in the *A. fragrans Willd.* Willd. leaf and stem extract that as agent of stabilizing were adsorbed on the surface AgNPs. Other impurities were not observed in EDX profile.

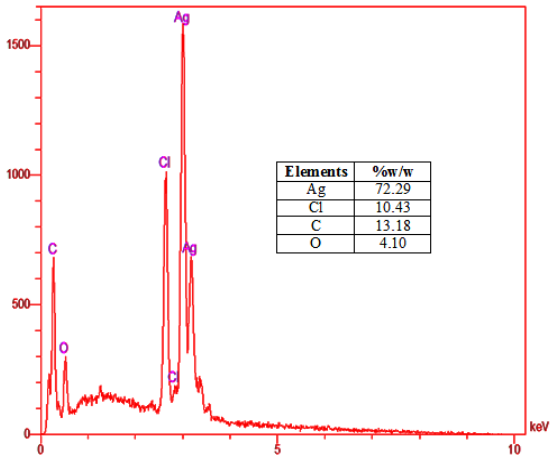

Figure 6. *EDX pattern for AgNPs synthesized based on MI (900 W) approach. The vertical axis displays the number of X-ray counts while the horizontal axis displays energy in keV.*

3.6. FTIR Characterization

Previous works revealed that the major compounds of the *A. fragrans Willd.* extract were carvone, mentha-1, 4, 8-triene, trans-chrysanthenyl acetate, isobornyl acetate and flavonol 3-methyl ether glucosides [30]. Therefore, the bio-capping of silver cations can occur in presence of these compounds which adhered to the surface of AgNPs. As

shown in Figure 7a-c, the spectra shows two bands at 3652.94 and 3739.28 cm^{-1} which attribute to the typical peaks of stretching O-H group of H-bonded phenolic moieties. The FTIR spectrum of the AgNPs shows two sharp bands at 2853.94 and 2925.31 cm^{-1} which attributes to -CH symmetric and asymmetric stretching of methylene group, respectively. The small sharp bands 1741.39 and 1652.97 cm^{-1} are assigned to the stretching vibrations of C=O and C=C, respectively. The band appeared at 1071.25 cm^{-1} could be due to -C-O stretching.

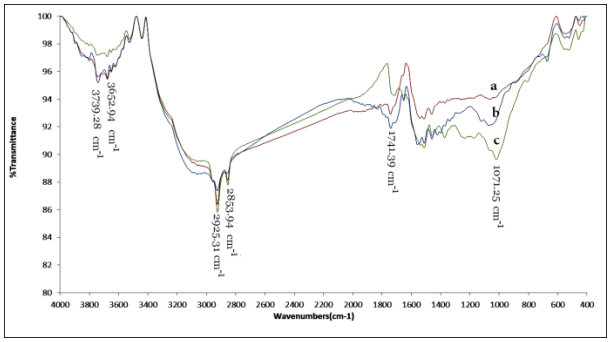

Figure 7. *Comparison of FTIR spectra for AgNPs synthesized by a) CH (100ºC), b) A. fragrans Willd. Willd. leaf and stem extract and c) MI (900 W).*

These data show the presence of the several functional groups in the extract which will be discussed in possible mechanism section. Thus, it appears that the secondary metabolites of the extract, such as flavonol 3-methyl ether glucosides, could be as a capping and stabilizing agent of AgNPs to avoid agglomeration [26]. These compounds play important role for the reduction of Ag^{+} to Ag^{0} and also stabilizing AgNPs. The carbonyl groups and π bonds of these compounds have a strong affinity to bind metals then can act as encapsulating agent and thus prevent the agglomeration of AgNPs [28, 31].

3.7. Performance at the Structural Chemistry

The free radical scavenging and possible mechanism in order to preparing of the AgNPs were evaluated in the present study.

a) Antioxidant property of the AgNPs

DPPH is a stabled nitrogen-containg free radical and shows a typical absorption peak at 517 nm. It shows a color changes from violet to yellow upon reduction. The free radical scavenging behavior of as-synthesized AgNPs and extract is seen in Figure 8. The antioxidants present in the AgNPs react with DPPH and convert it to 1,1-diphenyl-2-picryl hydrazine with decolorization. Therefore, it is possible to propose on equation (2):

AgNPs+DPPH→AgONPs+1,1-diphenyl-2-picrylhydrazine Eq. 2

In one hand, the scavenging percent of DPPH increases approximately in linear way with increase in the concentration of the AgNPs. On the other hand, it appears that the trend of the scavenging percent is as CH › MI › extract.

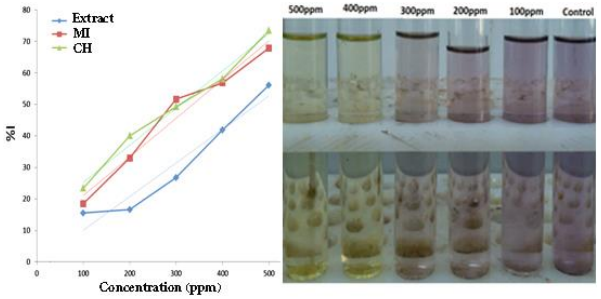

Figure 8. *DPPH scavenging by 100-500 ppm of AgNPs. Results represent mean scavenging±S.D.of triplicate determination*

As previously mentioned, the anti-oxidant molecules of the *A. fragrans Willd.* act synergistically. During the synthesis of AgNPs, these metabolites are pooled into the system. Therefore, these anti-oxidant molecules like flavonol 3-methyl ether glucosides may get adsorbed onto the bio-nano interface of the AgNPs. With considering the high surface area to volume ratio of AgNPs, they provide a high tendency to reduce DPPH radicals. Amusingly, such performance has recently

reported on the anti-oxidant activity of iron oxide particles as a surface dependent property [31].

b) Possible Mechanism

Although the exact mechanism for the phytosynthesis of metal oxide NPs using plant extracts has not been confirmed, but it was recommended that polar groups are responsible for the synthesis of NPs [32]. Figure 9 shows the proposed mechanism for the capping effect of the extract.

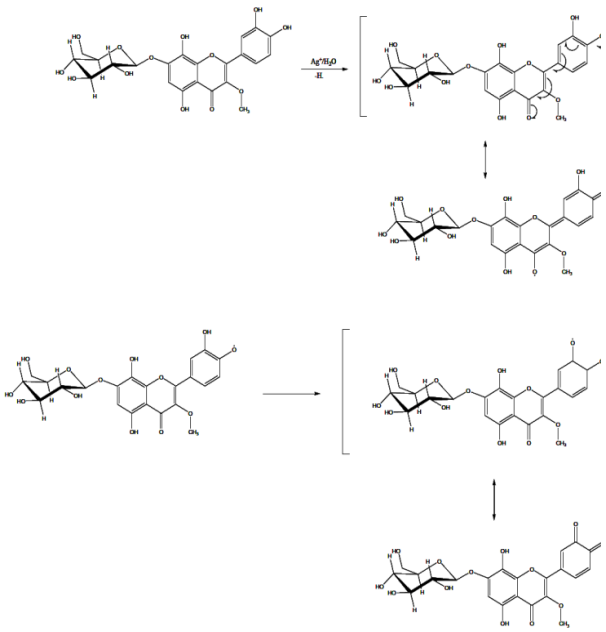

Figure 9. *The possible mechanism for the formation and stability of AgNPs.*

It appears that the lone pair electrons in the polar groups of flavonol 3-methyl ether glucosides can occupy orbital of the Ag^+, firstly. In the second stage, Ag^+ is capped with polar groups to form a complex compound inside the nanoscopic templates of metabolites.

4. CONCLUSION

In this research, we have compared both CH and MI methods for phytosynthesis of AgNPs using *A. fragrans Willd.* leaf and stem extracts. Both methods are nontoxic, low cost and clean which are in accordance with the green chemistry principles. As a result, in MI approach AgNPs were synthesized at a shorter time and smaller size than CH approach. The size of AgNPs synthesized by MI method was smaller than 100 nm. In conclusion, it was mentioned that MI technique is a cheap, fast and convenient technique suitable for commercial production as well as health related applications of AgNPs.

ACKNOWLEDGEMENT

The financial support by the Research institute for fundamental sciences (RIFS), University of Tabriz is gratefully acknowledged.

REFERENCES

1. Jafarirad, S., (2015). "*Dendritic architectures: Therapeutics*, Encyclopedia of Biomedical Polymers and Polymeric Biomaterials", 1st ed. Taylor & Francis Group, New York.
2. Jafarirad, S., (2015). "*Dendritic architectures: Theranostic agents*, Encyclopedia of Biomedical Polymers and Polymeric Biomaterials", 1st ed. Taylor & Francis Group 2015, New York.
3. Prow, T. W., Grice, J. E., Lin, L. L., Faye, R., Butler, M., Becker, W., Wurm, E. M., Yoong, C., Robertson, T. A., Soyer, H. P., (2011). "Nanoparticles and microparticles for skin drug delivery", *Advanced drug delivery Reviews*, 63: 470-491.
4. Chaudhry, Q., Castle, L., (2011). "Food applications of nanotechnologies: An overview of opportunities and challenges for developing countries", *Trends in Food Science & Technology*, 22: 595-603.
5. Nair, R., Varghese, S. H., Nair, B. G., Maekawa, T., Yoshida, Y., Kumar, D. S., (2010). "Nanoparticulate material delivery to plants", *Plant science*, 179: 154-163.
6. Kelly, F. M., Johnston, J. H., (2011). "Colored and Functional Silver Nanoparticle-Wool Fiber Composites", *ACS applied materials & interfaces*, 3: 1083-1092.
7. Dankovich, T. A., Gray, D. G., (2011). "Bactericidal paper impregnated with silver nanoparticles for point-of-use water treatment", *Environmental science & technology*, 45: 1992-1998.
8. Sharma, V. K., Yngard, R. A., Lin, Y., (2009). "Silver nanoparticles: green synthesis and their antimicrobial activities", *Advances in colloid and interface science*, 145: 83-96.
9. Song, J. Y., Kim, B. S., (2009). "Rapid biological synthesis of silver nanoparticles using plant leaf extracts", *Bioprocess and biosystems engineering*, 32: 79-84.

10. Darroudi, M., Ahmad, M. B., Shameli, K., Abdullah, A. H., Ibrahim, N. A., (2009). "Synthesis and characterization of UV-irradiated silver/montmorillonite nanocomposites", *Solid State Sciences*, 11: 1621-1624.
11. Darroudi, M., Ahmad, M., Zamiri, R., Abdullah, A., Ibrahim, N., Sadrolhosseini, A., (2011). "Time-dependent preparation of gelatin-stabilized silver nanoparticles by pulsed Nd: YAG laser", *Solid State Sciences*, 13: 520-524.
12. Aihara, N. Torigoe, K. Esumi, K., (1998). "Preparation and characterization of gold and silver nanoparticles in layered laponite suspensions", *Langmuir*, 14: 4945-4949.
13. Oluwafemi, O. S., Lucwaba, Y., Gura, A., Masabeya, M., Ncapayi, V., Olujimi, O. O., Songca, S. P., (2013). "A facile completely 'green'size tunable synthesis of maltose-reduced silver nanoparticles without the use of any accelerator", *Colloids and Surfaces B: Biointerfaces*, 102: 718-723.
14. El-Rafie, M., El-Naggar, M., Ramadan, M., Fouda, M. M., Al-Deyab, S. S., Hebeish, A., (2011). "Environmental synthesis of silver nanoparticles using hydroxypropyl starch and their characterization", *Carbohydrate Polymers*, 86: 630-635.
15. Vasileva, P., Donkova, B., Karadjova, I., Dushkin, C., (2011). "Synthesis of starch-stabilized silver nanoparticles and their application as a surface plasmon resonance-based sensor of hydrogen peroxide", *Colloids and Surfaces A: Physicochemical and Engineering Aspects*, 382: 203-210.
16. Shams, S., Pourseyedi, S., Hashemipour Rafsanjani, H., (2014). "Green Synthesis of Silver Nanoparticles and Its Effect on Total Proteins in Melia Azedarach Plant", *International Journal of Nanoscience and Nanotechnology*, 10: 181-186.
17. Mohammadinejad, R., Pourseyedi S., Baghizadeh A., Ranjbar S., Mansoori, G. A., (2013). "Synthesis of Silver Nanoparticles Using Silybum Marianum Seed Extract", *International Journal of Nanoscience and Nanotechnology*, 9: 221-226.
18. Jafarirad, S., Kordi, M., Kosari-Nasab, M., (2017). "Extracellular one-pot synthesis of nanosilver using Hyssopus officinalis L.:A biophysical approach on bioconstituent-Ag^{+} interactions", *INORGANIC AND NANO-METAL CHEMISTRY*, 47: 632–638.
19. Sowbarnika, R., Anhuradha, S., Preetha, B., (2018). "Enhanced Antimicrobial Effect of Yeast Mediated Silver Nanoparticles Synthesized From Baker's Yeast", *International Journal of Nanoscience and Nanotechnology*, 14: 33-42.
20. Kurian, M., Varghese, B., Athira, T. S., Krishna, S., (2016). "Novel and Efficient Synthesis of Silver Nanoparticles Using Curcuma Longa and Zingiber Officinale Rhizome Extracts", *International Journal of Nanoscience and Nanotechnology*, 12: 175-181.
21. Rasoulpour, I., Jafarirad, S., (2017). "Synthesis of biocapped CuO nanoparticles: An investigation on biorganic-Cu^{2+} interactions, in vitro antioxidant and antimicrobial aspects", *INORGANIC AND NANO-METAL CHEMISTRY*, 47: 1599–1604.
22. Delazar, A., Naseri, M., Nazemiyeh, H., Talebpour, A. H., Imani, Y., Nahar, L., Sarker, S. D., (2007). "Flavonol 3-methyl ether glucosides and a tryptophylglycine dipeptide from *Artemisia fragrans* (Asteraceae)", *Biochemical systematics and ecology*, 35: 52-56.
23. Tan, R. X., Zheng, W. F., (1998) "Biologically active substances from the genus Artemisia", *Tang, Planta Med.*, 64: 295-302.
24. Salomoni, R., Léo, P., Montemor, A. F., Rinaldi, B. G., Rodrigues. M. F. A., (2017). "Antibacterial effect of silver nanoparticles in Pseudomonas aeruginosa", *Nanotechnol Sci Appl.*, 10: 115–121.
25. Abboud, Y., Eddahbi, A., El Bouari, A., Aitenneite, H., Brouzi, K., Mouslim, J., (2013). "Microwave-assisted approach for rapid and green phytosynthesis of silver nanoparticles using aqueous onion (Allium cepa) extract and their antibacterial activity", *Journal of Nanostructure in Chemistry*, 3: 1-7.
26. Iravani, S., Zolfaghari, B., (2013). "Green synthesis of silver nanoparticles using Pinus eldarica bark extract", *BioMed research international*, 2013.
27. Satishkumar, M., Sneha, K., Won, S., Cho, C., Kim, S., Yun, Y., (2009). "Cinnamon zeylanicum bark extract and powder mediated green synthesis of nano-crystalline silver particles and its antibacterial activity", *Colloids Surf. B: Biointerfac*e, 73: 332-338.
28. Bar, H., Bhui, D. K., Sahoo, G. P., Sarkar, P., Pyne, S., Misra, A., (2009). "Green synthesis of silver nanoparticles using seed extract of Jatropha curcas", *Colloids and Surfaces A: Physicochemical and Engineering Aspects*, 348: 212-216.
29. Lue, J. T., (2001). "A review of characterization and physical property studies of metallic nanoparticles", *Journal of physics and chemistry of solids*, 62: 1599-1612.
30. Movafeghi, A., Djozan, D., Torbati, S., (2010). "Solid-phase microextraction of volatile organic compounds released from leaves and flowers of Artemisia fragrans", followed by GC and GC/MS analysis, *Natural product research*, 24: 1235-1242.
31. Paul, S., Saikia, J. P., Samdarshi, S. K., Konwar, B. K., (2009). "Investigation of antioxidant property of iron oxide particlesby 1′-1′diphenylpicryl-hydrazyle (DPPH) method", Magn. Magn. Mater., 321: 3621.

32. Ganesh Babu, M., Gunasekaran, P., (2009). Production and structural characterization of crystalline silver nanoparticles from Bacillus cereus isolate", *Colloids and surfaces B: Biointerfaces*, 74: 191-195.